

Extremely Small Energy Gap in the Quasi-One-Dimensional Conducting Chain Compound $\text{SrNbO}_{3.41}$

C. A. Kuntscher,^{1,2} S. Schuppler,¹ P. Haas,² B. Gorshunov,^{2,*} M. Dressel,² M. Grioni,³ F. Lichtenberg,⁴ A. Herrnberger,⁴ F. Mayr,⁴ and J. Mannhart⁴

¹Forschungszentrum Karlsruhe, Institut für Festkörperphysik, D-76021 Karlsruhe, Germany

²Physikalisches Institut, Universität Stuttgart, Pfaffenwaldring 57, D-70550 Stuttgart, Germany

³Institut de Physique Appliquée, Ecole Polytechnique Fédérale, CH-1015 Lausanne, Switzerland

⁴Institut für Physik, EKM, Universität Augsburg, Universitätsstrasse 1, D-86135 Augsburg, Germany

(Received 23 March 2001; published 18 November 2002)

Resistivity, optical, and angle-resolved photoemission experiments reveal unusual one-dimensional electronic properties of highly anisotropic $\text{SrNbO}_{3.41}$. Along the conducting chain direction, we find an extremely small energy gap of only a few meV at the Fermi level. A discussion in terms of typical 1D instabilities (Peierls, Mott-Hubbard) shows that neither seems to provide a satisfactory explanation for the unique properties of $\text{SrNbO}_{3.41}$.

DOI: 10.1103/PhysRevLett.89.236403

PACS numbers: 71.10.Pm, 71.20.-b, 78.20.-e, 79.60.-i

A one-dimensional (1D) interacting electron system no longer exhibits the quasiparticles known from Fermi liquid theory and is instead a Tomonaga-Luttinger liquid (TLL) whose properties also include spin-charge separation and a power-law behavior of correlation functions [1]. This 1D theory does not, however, directly apply to *real* 1D materials since some coupling between the 1D entities (such as chains or similar) is always present, rendering the systems *quasi-1D* and facilitating 2D and 3D ordering effects. Real 1D materials are thus conducive to various instabilities masking the predicted TLL characteristics [2]. Electron-phonon coupling, for instance, can lead to a gapped charge-density wave (CDW) ground state (Peierls transition), and electron-electron interaction may cause the opening of a Mott-Hubbard (MH) gap at commensurate band filling.

Recently, a new quasi-1D material was synthesized [3] which belongs to the series $\text{SrNbO}_{3.5-x}$ of perovskite-related transition-metal oxides, with characteristics spanning a wide range: Depending on the oxygen stoichiometry, these niobium oxides exhibit quasi-1D metallic character ($x \approx 0.1$) [4] or ferroelectricity ($x = 0$) with a very high transition temperature [5]. In this Letter, we focus on the unusual electronic properties of the quasi-1D metallic compound $\text{SrNbO}_{3.41}$ which were determined by dc resistivity, optical spectroscopy, and angle-resolved photoemission (ARPES). Along the conducting chain direction, an extremely small energy gap of only a few meV, much smaller than for other quasi-1D compounds, is observed at the Fermi level. The gap is discussed in terms of a Peierls and a MH scenario.

$\text{SrNbO}_{3.41}$ single crystals of typical size $3 \times 2 \times 0.2 \text{ mm}^3$ were grown [3,6] by the floating zone melting technique. The precise oxygen content was determined thermogravimetrically. The analysis of the room temperature (RT) x-ray powder diffraction pattern indicates single-phase composition with lattice constants $a =$

3.99 \AA , $b = 5.67 \text{ \AA}$, and $c = 32.46 \text{ \AA}$, in good agreement with earlier work [7]. The basic structural building blocks are NbO_6 octahedra [see Fig. 1(a)] grouped into slabs which extend parallel to the (a, b) plane and for $\text{SrNbO}_{3.4}$ are five octahedra wide along c . Only along the a axis the octahedra are connected continuously via their apical oxygen atoms, forming 1D chains.

The dc resistivity of $\text{SrNbO}_{3.41}$ along the three axes was measured using a four-point configuration [6]. Polarized reflection measurements along the a and b axes were

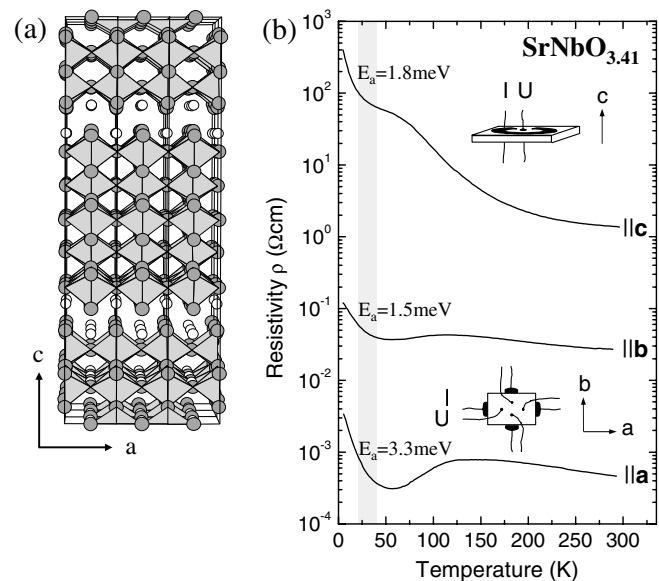


FIG. 1. (a) Projection along the b axis of the $\text{SrNbO}_{3.4}$ crystal structure; Nb atoms are hidden within the NbO_6 octahedra (light grey). White (grey) circles: Sr (O) atoms. (b) dc resistivity ρ versus temperature of $\text{SrNbO}_{3.41}$ along the three crystal axes, with the respective measurement geometry. In the range 20–40 K (grey bar), one finds an activated behavior $\rho \propto \exp\{E_a/k_B T\}$ with E_a as indicated.

performed for frequencies 6–34 000 cm^{-1} by utilizing various spectrometers; for details, see Ref. [8]. To accomplish the Kramers-Kronig analysis, we used a Hagen-Rubens extrapolation for $\omega \rightarrow 0$ and a power law (ω^{-4}) at high frequencies. High-resolution ($\Delta E = 15$ meV) ARPES data were recorded with a Scienta ESCA-300 analyzer using the He I α line of a discharge lamp. The samples were cleaved at RT and a base pressure of 1×10^{-10} mbar to expose an (001) surface, and cooled down to 25 K. By Laue diffraction, the crystals were oriented to $\pm 1^\circ$. The angular resolution was set to $\pm 0.5^\circ$, and the Fermi level E_F was determined to 1 meV accuracy from the Fermi cutoff of a freshly evaporated Au film recorded immediately afterwards at the same experimental conditions.

Figure 1(b) shows the dc resistivity ρ versus temperature T of $\text{SrNbO}_{3.41}$ along the three axes. It is highly anisotropic with very low, metal-like values along the a direction [$\rho_a(300\text{ K}) = 4.6 \times 10^{-4} \Omega \text{ cm}$] and a RT anisotropy of $\rho_a:\rho_b:\rho_c = 1:10^2:10^4$. The variation of ρ with temperature is smaller within the (a, b) plane than along c . In all directions, a broad maximum or shoulder is seen between 200 and 50 K, and below 50 K we find an increase of ρ , which in the range 20–40 K can be described by an activated behavior $\rho \propto \exp\{E_a/k_B T\}$ with activation energies $E_a = 2\text{--}3$ meV. In the range 60–130 K, ρ_a (along the chains) has a metallic T dependence, whereas above 130 K it slightly decreases with increasing temperature (thermally activated hopping between metallic strands may explain this). A similar temperature dependence is observed for ρ_b ; however, not as clearly developed. There are no signs of metallic behavior along c .

The anisotropy in the electrical properties of $\text{SrNbO}_{3.41}$ is also clearly seen in the optical response (Fig. 2). The reflectivity R displayed in the insets of Fig. 2 shows a sharp plasma edge for the polarization $\mathbf{E}||a$ with high values ($R \approx 1$) at low frequencies, indicating metallic conductivity. In contrast, for $\mathbf{E}||b$ the material is insulating, and we mainly see phonon contributions between 40 and 1000 cm^{-1} showing significant changes with temperature which will be discussed elsewhere [8]. For both polarization directions, the low frequency ($\omega \rightarrow 0$) conductivity σ_1 agrees, in general, well with the measured dc data (Fig. 1), reproducing its rather complicated temperature behavior. At RT, the $\mathbf{E}||a$ conductivity contains a Drude-like contribution at low frequencies followed by several phonon lines between 100 and 1000 cm^{-1} and a broad midinfrared band around 1500 cm^{-1} . Upon reducing the temperature, σ_1 exhibits substantial changes at frequencies lower than 100 cm^{-1} , leading to the appearance of a peak around 40 cm^{-1} which is already quite strong at 50 K. At 5 K, this peak has shifted slightly to higher frequencies and has grown even stronger. We ascribe this feature to single-particle excitations across an energy gap in the electronic density of states with $2\Delta(5\text{ K}) \approx 5$ meV.

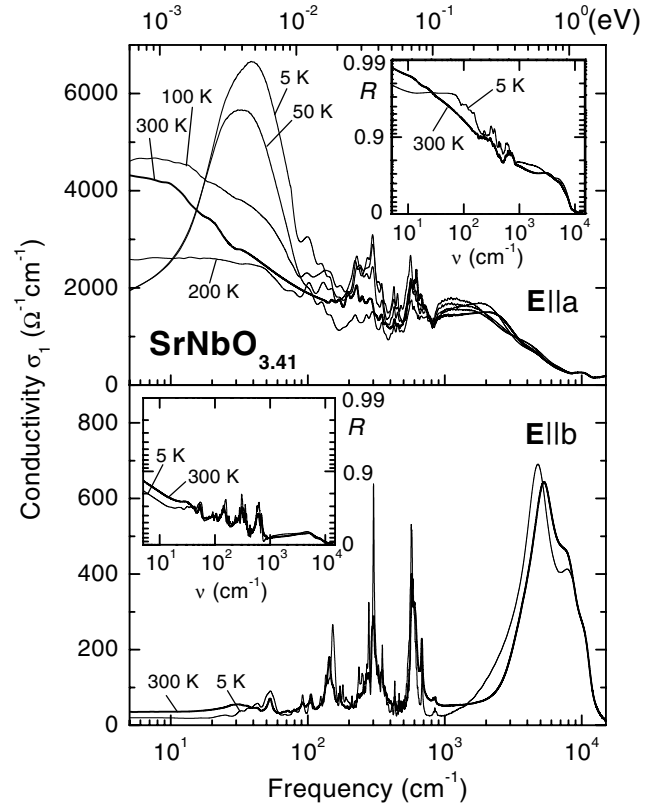


FIG. 2. Frequency dependent conductivity of $\text{SrNbO}_{3.41}$ for different temperatures and the polarization \mathbf{E} set parallel to the a and b axes (insets: reflectivity R used for Kramers-Kronig analysis). For $\mathbf{E}||a$, the low-temperature peak around 40 cm^{-1} indicates excitations across a gap $2\Delta \approx 5$ meV.

The momentum resolved electronic properties probed by ARPES reveal a quasi-1D band structure for $\text{Sr}_{0.9}\text{La}_{0.1}\text{NbO}_{3.39}$ [4] as well as for $\text{SrNbO}_{3.41}$ [8]: A dispersing band is found only along *one* high-symmetry line, $\bar{\Gamma}-\bar{X}$, parallel to the chain direction a , and seems to cross E_F ; a second band near E_F does not show discernible dispersion. Neither band disperses along the transverse direction $\bar{\Gamma}-\bar{Y}$. The Fermi surface (FS) is 1D [4], with nesting vector $2k_F$ of about $1/3$ of the Brillouin zone.

Further insight is gained by band structure calculations in the local density approximation [4,9] which demonstrate that among the three inequivalent Nb sites per slab a predominant [9] contribution to the density of occupied states at E_F comes from the *central* Nb site; the contributions of the other two Nb sites rapidly fall off with distance away from the center. Distortion is small only for the NbO_6 octahedra based on the central Nb sites, and one can thus clearly relate the quasi-1D character of the dispersing band to these chains of almost “perfect” octahedra in the middle of the slabs. The importance of the central chains is also demonstrated by comparing ARPES results for $\text{SrNbO}_{3.41}$ with those for $\text{Sr}_{0.8}\text{La}_{0.2}\text{NbO}_{3.50}$ [8], where the central chains are missing since there the slabs are only *four* octahedra wide: For the latter, the 1D character of the band structure has almost vanished.

The quasi-1D FS with almost complete nesting makes $\text{SrNbO}_{3.41}$ prone to instabilities opening a gap at E_F , and we thus concentrate on the region around k_F in order to very sensitively detect such signatures. Figure 3(a) shows the corresponding high-resolution ARPES spectra along $\bar{\Gamma}-\bar{X}$ near E_F . At $\Delta\theta = -1.5^\circ$, the peak associated with the strongly dispersing band is located at ≈ 160 meV binding energy and is rather broad, but sharpens up as it approaches E_F and appears to cross it. We define k_F ($\Delta\theta \equiv 0^\circ$) as the emission direction for which the leading edge midpoint of the spectrum is closest to E_F . Because of a 2×1 superstructure [4], the peak reappears already at $k_F^* = 5.5^\circ$ and disperses towards higher binding energies for increasing $\Delta\theta$. Figure 3(b) depicts the ARPES spectra around k_F for a narrow angular step size of 0.25° together with the Fermi cutoff of a Au film. Starting from -0.5° and going to higher $\Delta\theta$, the leading edge midpoint approaches E_F but *does not reach it* for any of the spectra. At k_F , the spectral weight at the Fermi level is significantly suppressed (by $\approx 40\%$) compared to the leading edge midpoint, and we find a gap between the leading edge midpoint and E_F of $\Delta(25 \text{ K}) \approx 4$ meV. Although this “leading edge” method is known to underestimate

the gap size somewhat for a peaklike structure, a fit (not shown) of the k_F spectrum, similar to Ref. [10] and accounting for the peak structure, gives only a slightly larger result, $\Delta(25 \text{ K}) \approx (5 \pm 2)$ meV, corroborating the leading edge result. Possible extrinsic effects such as charging or too coarse an angular step size can also be excluded as a source of the gap [11]. The gap is thus clearly established and with a size of about 5 meV is, in fact, the smallest one found in ARPES for any quasi-1D compound.

The intensity plot of high-resolution ARPES spectra in 0.5° steps and normalized for clarity to constant total intensity is shown in Fig. 3(c). It indicates additional states between k_F and k_F^* , where the strongly dispersing band is unoccupied: Beyond k_F a “shadow band” is visible which disperses away from the gap edge and exhibits a symmetry consistent with the 2×1 superstructure. Its small intensity is compatible with the small gap size [12]. As shadow bands are rather weak in general a clear identification in experiment has been possible only for very few quasi-1D materials [12,13].

The different experiments on $\text{SrNbO}_{3.41}$ all yield clear evidence for an energy gap at E_F along the conducting chains: a rise in the dc resistivity, a strong peak in the optical conductivity, as well as a significant suppression of spectral weight in ARPES. All results lead to characteristic energies of a few meV — agreeing well enough to demonstrate that the gap does exist and suggesting a common origin. Some spread is present, as expected, due to the different nature of the excitation for the various techniques (the optical gap, e.g., is somewhat smaller, possibly due to excitonic effects).

Most surprising is the gap’s *extreme smallness*, making it unique among quasi-1D materials; the unusual properties of the gap, however, turn out to defy easy explanation: (i) A lattice superstructure with sufficiently small displacement amplitudes would, of course, be able to reproduce the gap and its small size. It *cannot*, however, plausibly explain why the gap should be situated right at E_F , considering the large width (≥ 2 eV [4,9]) of the quasi-1D band. The instabilities of quasi-1D systems, on the other hand, by their very nature cause a gap located at E_F and thus are more likely candidates for an explanation of the gap properties observed for $\text{SrNbO}_{3.41}$ — such as (ii) a MH-type insulating state with a gap at E_F due to electron-electron interaction; for this, the filling level of the quasi-1D band would have to be commensurate, $1/3$. This $1/3$ filling, however, would require long-range interaction and a TLL parameter $K_\rho < 1/3$ for a MH gap to open [14], and the very strong correlation implied by the latter appears implausible for $\text{SrNbO}_{3.41}$: Correlation effects are generally small for $4d$ systems such as niobium oxides. The possibility of a MH gap is thus unlikely yet cannot be fully excluded based on our data as theoretical results for $1/3$ filling are still scarce. (iii) A Peierls instability caused by electron-phonon coupling appears possible, too, leading to a CDW

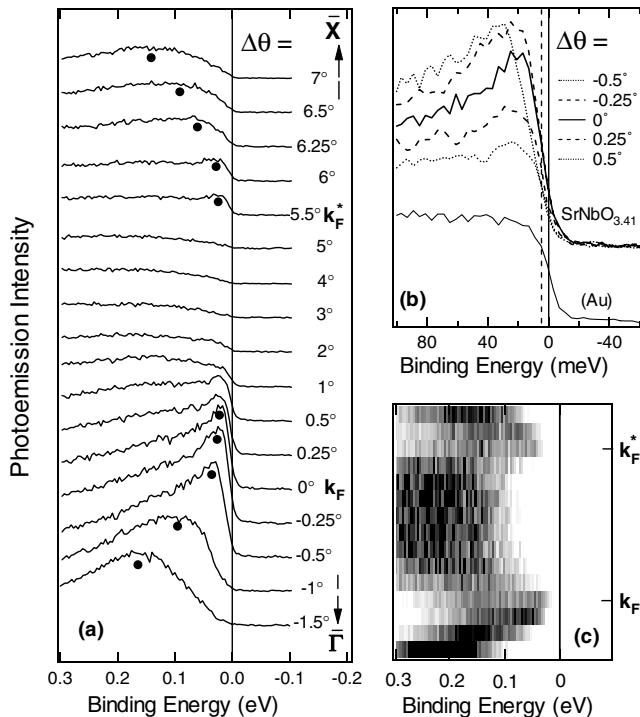


FIG. 3. ARPES spectra of $\text{SrNbO}_{3.41}$ along $\bar{\Gamma}-\bar{X}$ near k_F at $T = 25$ K. The angle $\Delta\theta$ is the emission angle with respect to k_F ($\Delta\theta \equiv 0^\circ$). (a) Spectra between the two “crossing points” (k_F , k_F^*) of the strongly dispersing band; peak positions are marked by dots. (b) Spectra around k_F in 0.25° steps. A gap $\Delta \approx 5$ meV is seen when compared to the Fermi cutoff of a gold film (thin solid line). (c) Intensity plot of spectra, taken between k_F and k_F^* (step size 0.5°) and normalized to constant total intensity; a weak, dispersing shadow band can be identified.

state for sufficiently low temperatures with a gap at E_F [15,16]. The gap size is related to the mean-field (MF) transition temperature T_P^{MF} , and in the weak-coupling limit $2\Delta(0) = 3.52k_B T_P^{\text{MF}}$; from the ARPES gap $2\Delta(25 \text{ K}) \approx 10 \text{ meV}$, one can then estimate $T_P^{\text{MF}} \approx 40 \text{ K}$ [17]. *Only below* this temperature the gap (or its precursor, the fluctuation-induced pseudogap) can exist; in this sense T_P^{MF} strictly limits the temperature range where any gap-related features can possibly be observed. Yet, for $\text{SrNbO}_{3.41}$ one clearly sees the upturn in $\rho_a(T)$ (Fig. 1) to start at $\approx 55 \text{ K}$, and the low-energy peak for $\mathbf{E}||a$ in optics (Fig. 2) is almost fully developed already at 50 K , suggesting an onset well above that temperature. A simple Peierls picture therefore is also insufficient to provide an explanation for the observed small gap [18]. Inconsistencies between the experimental results and theoretical models have been found for other quasi-1D systems as well, such as the paradigmatic $(\text{NbSe}_4)_3\text{I}$, $(\text{TaSe}_4)_2\text{I}$, and $\text{K}_{0.3}\text{MoO}_3$. The latter two are CDW systems yet show clear discrepancies to the Peierls picture (e.g., ARPES line shape and Fermi cutoff above T_P), which were attributed to correlation effects [2,19]. In contrast, quasi-1D $\text{SrNbO}_{3.41}$ has no obvious Peierls transition, little tendency to correlation, and the relevant energy scale is drastically smaller. It seems to be a system with characteristics distinctly its own, thus expanding the parameter space where real 1D systems remain to be fully understood.

In summary, we consistently observe in ARPES, dc resistivity, and optics that $\text{SrNbO}_{3.41}$ is a compound with 1D electronic characteristics around E_F ; as expected for such a system, instabilities lead to an energy gap at E_F . Most surprising is its small gap size: only a few meV by all techniques and thus much smaller than for other quasi-1D compounds. Further analysis shows the experimental findings to appear inconsistent with validity ranges for both the Peierls and Mott-Hubbard picture. These aspects promise more general implications for the understanding of *real* 1D systems.

We thank B. Götz, G. Hammerl, A. Loidl, L. Perfetti, C. Rojas, C. Schneider, R. Schulz, I. Vobornik, J. Voit, and H. Winter for valuable help and fruitful discussions. This work was supported by the DAAD, the BMBF (Project No. 13N6918/1), and the DFG.

*Permanent address: General Physics Institute, Academy of Sciences, Vavilov 38, Moscow 117942, Russia.

[1] J. Voit, Rep. Prog. Phys. **58**, 977 (1995).

- [2] M. Grioni and J. Voit, in *Electron Spectroscopies Applied to Low-Dimensional Materials*, edited by H. P. Hughes and H. I. Starnberg (Kluwer, Dordrecht, 2000).
- [3] F. Lichtenberg *et al.*, Z. Phys. B **84**, 369 (1991); T. Williams *et al.*, J. Solid State Chem. **103**, 375 (1993).
- [4] C. A. Kuntscher *et al.*, Phys. Rev. B **61**, 1876 (2000).
- [5] S. Nanamatsu *et al.*, J. Phys. Soc. Jpn. **30**, 300 (1971); S. Nanamatsu, M. Kimura, and T. Kawamura, J. Phys. Soc. Jpn. **38**, 817 (1975).
- [6] F. Lichtenberg *et al.*, Prog. Solid State Chem. **29**, 1 (2001).
- [7] S. C. Abrahams *et al.*, Acta Crystallogr. Sect. B **54**, 399 (1998).
- [8] C. A. Kuntscher *et al.* (to be published).
- [9] H. Winter, S. Schuppler, and C. A. Kuntscher, J. Phys. Condens. Matter **12**, 1735 (2000).
- [10] N. P. Armitage *et al.*, Phys. Rev. Lett. **86**, 1126 (2001).
- [11] Charging: With $\rho_{a,b,c}$ (25 K) from Fig. 1, estimates of possible charging effects induced by the total photoemission current turn out to be 3 orders of magnitude smaller than the gap size observed. Angular step size: Simulated ARPES spectra within the Fermi liquid model for a band with the experimental dispersion near k_F and accounting for the experimental angular and energy broadening show that (i) the gap indeed *closes* at k_F , and that (ii) a step size of 0.25° (implying that the actual k_F can be "missed" by 0.125° at most) is clearly sufficient to rule out that a gap with $\Delta > 1 \text{ meV}$ could be due to this effect.
- [12] J. Voit *et al.*, Science **290**, 501 (2000).
- [13] V. Vescoli *et al.*, Phys. Rev. Lett. **84**, 1272 (2000); J. Schäfer *et al.*, *ibid.* **87**, 196403 (2001).
- [14] H. J. Schulz, in *Strongly Correlated Electronic Materials*, edited by K. S. Bedell *et al.* (Addison-Wesley, Reading, MA, 1994).
- [15] R. Peierls, *Quantum Theory of Solids* (Oxford University Press, London, 1955).
- [16] The fact that no signatures for a transition are obvious in resistivity (Fig. 1) or detectable in thermal expansion [P. Nagel, V. Pasler, and C. Meingast (unpublished)] may be due to the low number of electrons involved in the 1D character of $\text{SrNbO}_{3.41}$; it does not by itself mean that a Peierls transition does not occur.
- [17] A BCS-type approximation for $\Delta(T)$ was used for the estimate.
- [18] The structural affinity of $\text{SrNbO}_{3.41}$ to ferroelectric $\text{SrNbO}_{3.50}$ may be of importance: The central chains responsible for the 1D electronic character are coupled to a network of polarizable NbO_6 octahedra structurally equivalent to those giving rise to the high dielectric constant in the ferroelectric, and a certain influence on the electronic properties of the chains is conceivable.
- [19] L. Perfetti *et al.*, Phys. Rev. Lett. **87**, 216404 (2001).